RESEARCH PAPER

Resveratrol-loaded cumin seed oil nanoemulsion ameliorates neurodegeneration in mice by inhibiting apoptosis, inflammation, and oxidative DNA damage

Shaymaa M. Eissa [1], Mohamed S. Elsayed [1], Azza M. Gawish [1], Heba E. Elzorkany [2], Salwa Sabet [1]*

[1]*Department of Zoology, Faculty of Science, Cairo University, Giza 12613, Egypt*
[2]*Nanotechnology and Advanced Materials Central Lab, Agriculture Research Center, Egypt*

ABSTRACT

Objective(s): Neurodegenerative diseases affect over 50 million people worldwide. Unfortunately, there are no cures for these diseases, so finding effective treatments to improve human health is crucial. Resveratrol (Res) has neuroprotective effects due to its antioxidant and anti-inflammatory properties. However, Res is limited by poor water solubility and bioavailability. Therefore, the current study aimed to overcome Res's limitations using recent nanotechnology.

Materials and Methods: Resveratrol was loaded onto a nanoemulsion of cumin seed oil (CSONEs). The CSONEs and Res-CSONEs were characterized. Additionally, we investigated the neuroprotective effects of Res-loaded CSONEs in mice with Trimethyltin (TMT)-induced neurodegeneration. Thirty mice were divided into control, vehicle, TMT, TMT-CSONEs, TMT-Res, and TMT-Res-CSONEs. Each group received intraperitoneal treatment six times per week for two weeks. oxidative stress biomarkers, DNA damage extent, and histopathological evaluations were assessed in brain and liver tissues. In addition, the mRNA expression of apoptotic and inflammatory genes (Bax/Bcl2 and il-1β) and immunohistochemical staining of tau protein were evaluated in the brain tissues.

Results: The Res-CSONEs improved cellular homeostasis by increasing GSH, and SOD, and decreasing MDA levels while decreasing the DNA damage parameters. They also decreased the expression of apoptotic and inflammatory genes and reduced the aggregation of tau protein. Histopathological examination of the studied tissues showed improvement in Res and Res-CSONEs compared to TMT.

Conclusion: Loading Res on CSONEs resulted in promising neuroprotective effects due to its solubility and bioavailability enhancement. Combining the antioxidant and anti-inflammatory properties of both Res and CSONEs resulted in perfect neuroprotective effects on the brain tissues of mice.

Keywords: *Inflammation, Mice, Nanoemulsions, Neurodegeneration, Resveratrol*

How to cite this article
Eissa ShM, Elsayed MS, Gawish AM, Elzorkany HE, Sabet S. Resveratrol-loaded cumin seed oil nanoemulsion ameliorates neurodegeneration in mice by inhibiting apoptosis, inflammation, and oxidative DNA damage. Nanomed J. 2024; 11(4): 378-391. DOI: 10.22038/nmj.2024.75726.1841

INTRODUCTION

Neurodegenerative diseases such as Alzheimer's disease, Parkinson's disease, and Huntington's disease have had a highly negative impact on both global health and the economy. According to Alzheimer's Disease International, in 2021, an estimated 50 million people have been affected by Alzheimer's disease. It is also the sixth leading cause of death worldwide, causing around 1.6 million deaths in 2020 [1, 2]. Parkinson's disease, the second neurodegenerative disorder after Alzheimer's disease, affects over 6 million people worldwide [3]. The economic impact of Alzheimer's disease and other dementias has reached $1 trillion, while for Parkinson's disease, the economic cost was over $52 billion in 2019 [2, 4]. This has placed a significant burden on healthcare systems and economies globally [1]. These statistics highlight the global burden of neurodegenerative diseases and emphasize the need for ongoing research, innovative therapies, and worldwide efforts to reduce the social,

* *Corresponding author: Email: shaymaa.doh2011@cu.edu.eg*
Note. This manuscript was submitted on October 24, 2023; approved on May 8, 2024

economic, and healthcare challenges associated with these debilitating conditions.

Resveratrol (Res) is a polyphenolic non-flavonoid compound naturally present in several plants such as red grapes, peanuts, green tea, and mulberries [5]. Administration of Res has been linked to a variety of therapeutic impacts, including analgesic, anti-inflammatory, anticarcinogenic, and antioxidant evidence [6]. As a result, Res has been investigated as a therapeutic agent for numerous diseases such as cardiovascular disease, obesity, diabetes, and more recently, neurological disorders such as brain tumors (gliomas), Alzheimer's (AD), and Parkinson's (PD) diseases [6-8]. Several recent studies illustrated the neuroprotective effect of RES against various neurodegenerative diseases via suppression of β-amyloid aggregation and oxidative stress suppression, and the prevention of apoptosis [9-11].

Although Resveratrol possesses enormous therapeutic promise, it suffers from several limitations due to its poor bioavailability, rapid metabolism and clearance, chemical instability, high photosensitivity, and poor water solubility [12, 13]. Due to its limited bioavailability, Res cannot reach the target tissue at the required amount for effective therapy [5]. Then, new approaches are necessary to overcome Res's limitations and realize the great benefits of its usage. Drug delivery systems, such as nanoparticles or nanoemulsions, can protect Res from metabolism and enhance its stability [13]. These delivery systems can also improve the solubility of Res, allowing for better distribution and accumulation in the target tissue [12].

Nanoemulsions (NE) are emulsions that are produced in nanometer sizes ranging from 10-200 nm and play an important role in the drug delivery system [14, 15]. This is achieved by enhancing the solubility of lipophilic drugs, improving the permeability and bioavailability of the drug as well as it can carry both hydrophilic and lipophilic drugs and protecting the drug from hydrolysis and oxidation [16-18]. Additionally, nanoemulsions (NE) are thermodynamically and kinetically stable, which renders them resistant to flocculation, creaming, sedimentation, and coalescence, and may be water-in-oil (w/o) or oil-in-water (o/w) formed by applying high or low external shear [15]. According to previous studies, several oil types are suitable in the preparation of nanoemulsions such as olive oil, corn oil, soyabean oil, sesame oil, coconut oil, rice bran oil, chia seed oil, cumin seed oil, orange oil, grape seed oil [19-23].

Cumin seed oil is an essential oil extracted from herbaceous plant from the Apiaceae family, characterized by a distinctive odor [24]. Cumin seed exhibits several pharmacological aspects such as antimicrobial, antidiabetic, antiepileptic, anticancerous, hepatoprotective, neuroprotective, antioxidant, anti-inflammatory, antifungal, and antibacterial [24-28]. From the previously illustrated benefits of cumin seed oil and Res, we will load Res on cumin seed oil nanoemulsion for the first time to combine their great benefits against neurodegenerative disease.

Trimethyltin (TMT) is a potent neurotoxicant, that causes neurodegeneration in the limbic system, particularly in the hippocampus in humans and animals [29, 30]. Exposure of both humans and animals to TMT leads to several neurodegenerative disorders, disorientation, ataxia, amnesia, aggressive behavior, and learning impairment [30]. TMT has been shown to induce neurodegeneration and cell death in certain brain regions, especially in the hippocampus [31], so it is used as a tool to investigate the cellular and molecular mechanisms of neurodegenerative diseases [32]. Therefore, in the current study, we aimed to investigate the neuroprotective effects of resveratrol-loaded cumin seed oil nanoemulsions against neurodegeneration in mice.

MATERIALS AND METHODS

All Experimental procedures were performed according to relevant guidelines and regulations.

Preparation of cumin seed oil nanoemulsions and Resveratrol-loaded cumin seed oil nanoemulsions

Cumin seed oil nanoemulsions (CSONEs) were prepared according to Nirmala, *et al*., method. Briefly, one ml of cumin seed oil was added to 2 ml of tween 80, then 13 ml water was added, the ratio of oil: tween 80: water was 1:2:13, and the solution was sonicated at 20 kHz for 10 min (probe-sonicator, Hielscher UP400St ultrasonic processor) [22].

As for the Res-loaded cumin seed oil nanoemulsions (Res-CSONEs), it was prepared following the same oil: tween 80: water ratios but with half the volume, according to Locatelli, *et al*., protocol. Briefly, 45 mg of resveratrol was added to 0.5 ml of cumin seed oil, and the mixture was sonicated using a water bath sonicator for 10 min. Then, 1 ml tween 80 was added and vortexed for 10 min, and finally, 6.5 ml water was added and, the solution was sonicated for 10 min using a probe-sonicator [21].

Characterization of CSONEs and Res-CSONEs

A high-resolution transmission electron

microscope (HR-TEM, Tecnai G20, FEI, Netherland) was used to detect the size and morphology of the cumin seed oil nanoemulsion and resveratrol-loaded cumin seed oil nanoemulsion, on an amorphous carbon-coated-copper grid and magnification power up to 1,000,000 X for imaging. TEM images were analyzed using Fiji and the average size was estimated depending on 60 particles from at least three different TEM images. Dynamic light scattering (DLS) was used to determine the hydrodynamic diameter of the nanoparticles and surface zeta potential was performed by Malvern Instruments Ltd, UK.

Experimental animals

A total of 30 mice ranging from 25-30 g in weight were obtained from the animal house of the National Cancer Institute in Egypt (NCI). Mice were housed in well-ventilated and sterilized cages (5 mice per group) under controlled temperature (20-25 ˚C), humidity, 12-hr light/dark cycle, and adapted for 6 days before the experiment. The experimental animal studies were performed in accordance with ARRIVE guidelines. In addition, the experimental protocol was approved by the Institutional Animal Care and Use Committee (CU-IACUC) at the Faculty of Science, Cairo University, with approval number (CU/I/F/16/21).

Experimental design and sample collection

Animals were divided into 6 groups as the following: Healthy control group, 2% ethanol group (vehicle), TMT group intraperitoneally administrated with 2.6 mg/kg TMT only once, TMT-CSONEs group was treated with 2.6 mg/kg TMT only once and 100 mg/kg of CSONEs one week before TMT and for two weeks after TMT administratiion, TMT-Res group was administrated 2.6 mg/kg TMT only once and 10 mg/kg of Res one week before TMT and for two weeks after TMT administtration, TMT-Res-CSONEs group was treated with 2.6 mg/kg TMT only once and 10 mg/kg of Res-CSONEs one week before TMT and for two weeks after TMT administration. All treatments were performed six times per week intraperitoneally [33-36]. 24 hr after the last treatment, mice were anesthetized and sacrificed by cervical dislocation. The brain and liver were immediately dissected and stored in an appropriate condition.

Assessment of oxidative stress biomarkers

According to the protocols outlined by Ohkawa *et al*, Beutler *et al*., and Nishikimi *et al*, 0.30g–0.45g of the examined tissues were homogenized in 50 mM phosphate buffer (pH: 7.4), centrifuged for 10 minutes at 3000 rpm at 4 ˚C, and the supernatants were used to measure Malondialdehyde (MDA), Superoxide dismutase (SOD) and Glutathione (GSH) [37-39].

Assessment of DNA damage using comet assay

Alkaline single-cell gel electrophoresis (SCGE) comet assay was used to measure the extent of DNA damage in both brain and liver tissues as described by [40, 41]. The prepared slides were examined by using an epifluorescence microscope (Leica, Germany) to image about 50 cells scored by using TriTek Comet Score™ Version 1.5 software. The DNA damage for each cell was determined according to three parameters: Tail length (TL) used to measure DNA damage that migrates from the nucleus, % of DNA in the tail, and Tail moment (TM).

Gene expression analysis

The brain samples that were conserved in RNA later (brand and company) and stored at -80 ˚C were used to assess the expression of *Bax, Bcl2, il-1β* and normalized using *GAPDH* as a housekeeping gene, primers were synthesized by Invitrogen (Carlsbad, CA, USA) and their sequences are shown in Table 1. Thermo Scientific GeneJET RNA purification kit

Table 1. Primers sequences used in quantitative real-time PCR analysis

Genes	Primers	Sequences (5'-3')	Bp	Accession No.
GAPDH	Forward	GTATCGGACGCCTGGTTAC	128bp	NM_001289726
	Reverse	CTTGCCGTGGGTAGAGTCAT		
il-1β	Forward	TGCCACCTTTTGACAGTGATG	138bp	NM_008361.4
	Reverse	TGATGTGCTGCTGCGAGATT		
Bax	Forward	GTCTCCGGCGAATTGGAGAT	100bp	NM_007527.3
	Reverse	ACCCGGAAGAAGACCTCTCG		
Bcl2	Forward	CATCGCCCTGTGGATGACTG	95bp	NM_009741.5
	Reverse	GGCCATATAGTTCCACAAAGGC		

(Thermo Scientific, USA) was used to extract cellular RNA from brain tissues of control and treated groups, according to kit's protocol. RevertAid First Strand cDNA Synthesis Kit (Thermo-Scientific, USA) was used for cDNA synthesis.

Finally, qPCR was performed according to kit instructions in a 25 µL reaction volume using PowerUp ™ SYBER™ Green Master Mix (applied biosystems) kit on a StepOnePlus Real-Time PCR System (Applied Biosystem, Foster City, CA, USA). The PCR program included an initial heat activation step at 95 °C for 15 min followed by 40 cycles of denaturation at 95 °C for 15 sec, annealing, and elongation at 60 °C for 1 min. Samples were analyzed in triplicates for each gene. Relative quantification of all genes was performed using the Comparative Ct method (ΔΔCT), which compares the expression of all genes with the expression of the reference gene.

Immunohistochemistry of tau protein

Immunohistochemical examinations of Tau protein were performed using the streptavidin-biotin method. Paraffin-embedded brain tissue sections, 5 microns thick, were prepared. The tissue sections were deparaffinized and treated with 0.3% H_2O_2 for 20 min. The brain samples were then incubated with anti-Tau protein (1:50 with TBS) for 2 hr. The tissue sections were washed with PBS and incubated with mouse horseradish peroxidase (HRP) [5 µg/ml (1:200)] (MAP kit, Medimabs, Canada) for 1 hr, then with diaminobenzidine (DAB) for 15 min. The sections were washed with PBS, counter-stained with hematoxylin, dehydrated, cleared in xylene, and cover-slipped for microscopic examination [42]. Six non-overlapping fields were randomly selected and scanned from the cortex and subiculum regions of the brain of each sample by an examiner histologist using a light microscope (Zeiss).

Estimation of histopathological alterations

Autopsy samples of the brain and liver were fixed in 10% formal saline for 24 hr. A serial series of alcohol was used for sample dehydration, then cleared in xylene and embedded in paraffin wax. Specimen blocks were sectioned at 4 microns thickness by rotary LEITZ microtome. specimen sections were collected on glass slides, deparaffinized, and stained by hematoxylin & eosin stain [43]. A light electric microscope (Zeiss, Germany) was used to examine slides for histopathological changes.

Statistical analysis

Statistical software package (IBM-SPSS) version 23 software was used to analyze the resultant data. According to the Shapiro-Wilk test, the data was normally distributed. Two-way ANOVA was applied to study the effect of treatment and their interaction with the studied variables. One-way ANOVA was used to illustrate the effect of treatment on the studied variables. Duncan's test was utilized to study the similarity among the experimental groups. The least significant difference (LSD) was used to check for significant differences among the studied groups.

RESULTS

Characterization of nanoemulsions

CSONEs and Res-CSONEs were characterized by using a transmission electron microscope (TEM), which revealed an average size of CSONEs and Res-CSONEs as 9.6 ±2.1 and 10.2±2.3 nm, respectively, and they appeared spherical in shape. The hydrodynamic diameter of approximately 100% of CSONEs and Res-CSONEs were (11.7 and 14.76 d.nm) with (pdl 0.356 and 0.470) respectively, which were determined by using dynamic light scattering (DLS). The Zeta potential of the nanoemulsions was -1.48 and -0.903 mV with zeta deviation (3.12 and 3.65 mV) in both of CSO-NEs and Res-CSONEs as in Fig. 1.

Ameliorative effect of Res-CSONEs on oxidative stress

The oxidative stress biomarkers MDA, GSH, and SOD were measured in the brain and liver tissues of all examined groups (Fig. 2 and 3). MDA levels were significantly ($P<0.05$) increased in the TMT group compared to all examined groups. In addition, the Res-CSONEs treated group appeared to have a significant ($P<0.05$) decrease in MDA level compared to both Res and CSONEs groups in the brain, which was near the control level. GSH content in the brain and hepatic tissues illustrated a significant ($P<0.05$) decrease in the TMT group compared to all groups, and a significant ($P<0.05$) increase in GSH content in the Res-CSONEs compared to CSONEs and Res group, which reflects an improvement in the oxidative stress environment due to the treatment with Res-

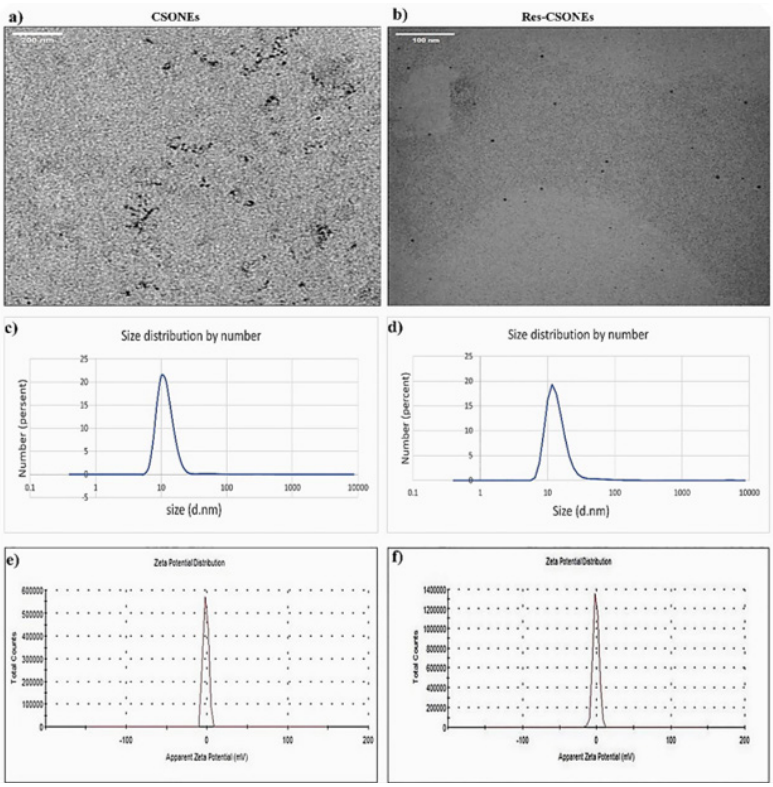

Fig. 1. Characterization of nanoemulsions (a&b) representative TEM micrograph showing CSONEs and Res-CSONEs with an average particle size= 9.6 ±2.1 and 10.2±2.3 nm, respectively. (c&d) The hydrodynamic diameter of 100% CSONEs and Res-CSONEs (11.7 and 14.76 d.nm). (e&f) represents the zeta potential measurements (-1.48 and -0.903 mV) of CSONEs and Res-CSONEs respectively

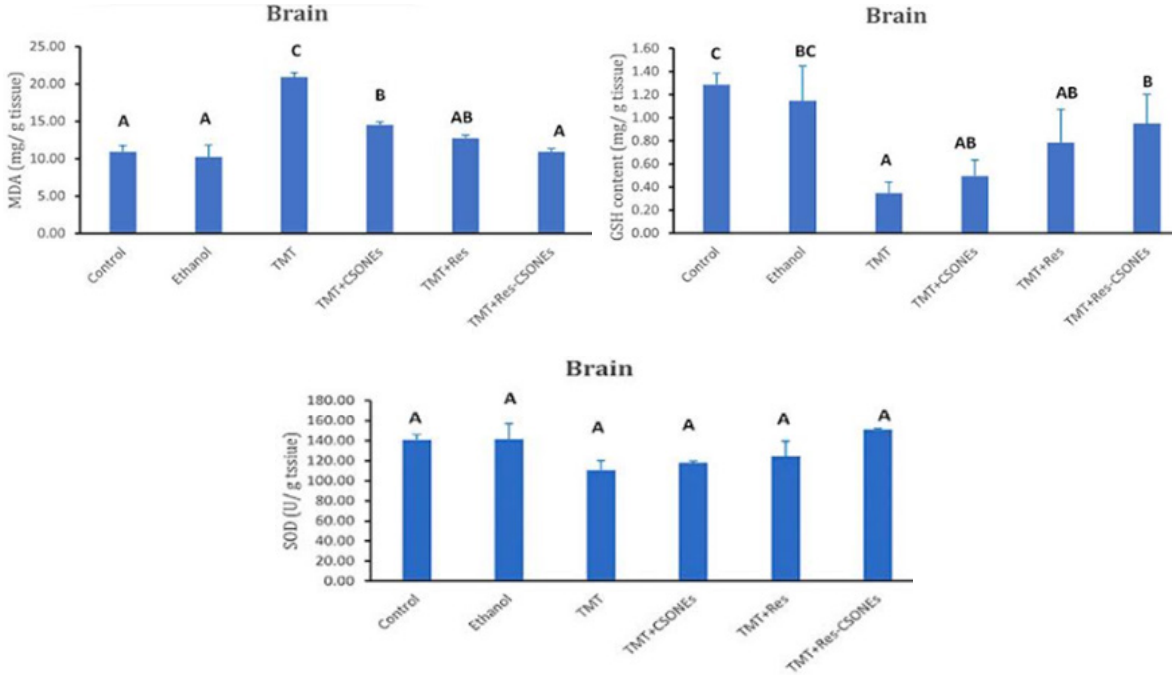

Fig. 2. The levels of malondialdehyde (MDA), glutathione (GSH), and superoxide dismutase (SOD) in the brain of the examined groups. Data are displayed as mean ± standard error. Bars labeled with the same superscript letters are insignificantly (P>0.05) different, whereas those marked with different ones are significantly (P<0.05) different

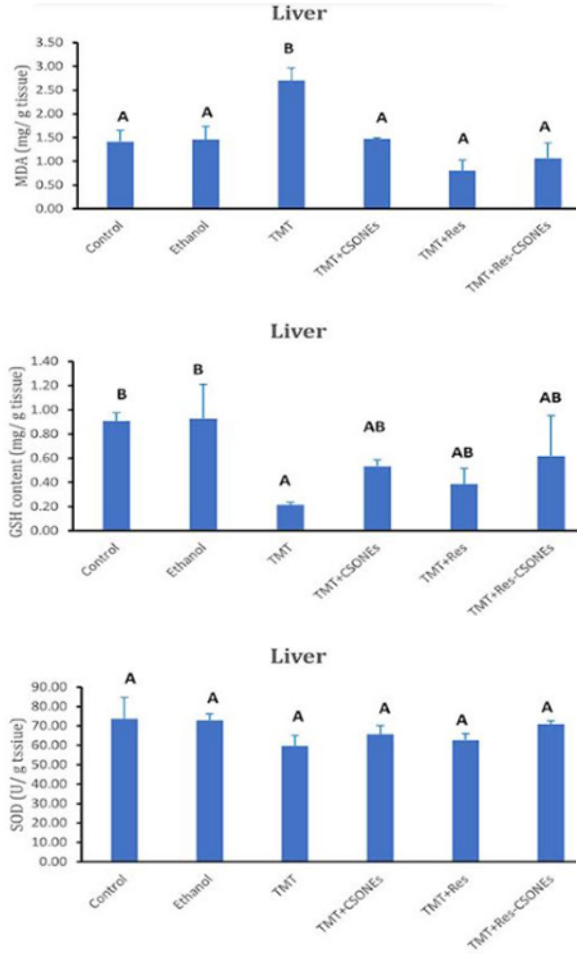

Fig. 3. The levels of malondialdehyde (MDA), glutathione (GSH), and superoxide dismutase (SOD) in the liver of the examined groups. Data are displayed as mean ± standard error. Bars labeled with the same superscript letters are insignificantly (P>0.05) different, whereas those marked with different ones are significantly (P<0.05) different

CSONEs. There is no significant (P>0.05) change in SOD activity in all treated groups in both brain and hepatic tissues.

Res-CSONEs reduced the extent of DNA damage

The amount of DNA damage in both brain and liver tissues of all the experimental groups was evaluated using the comet assay. In brain tissue, comet parameters TL, % DNA, and TM levels were significantly (P<0.05) increased in the TMT group compared to all examined groups. In addition, Res-CSONEs illustrated a significant (P<0.05) reduction in all comet parameters compared to Res and

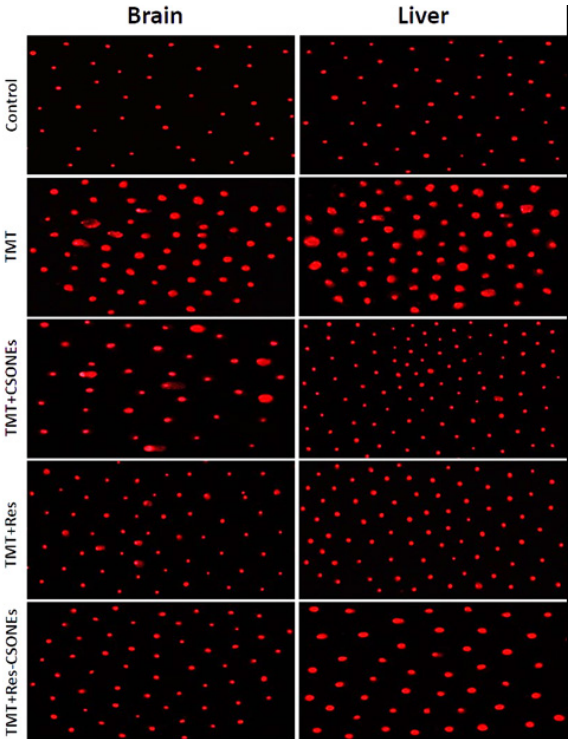

Fig. 4. Representative fluorescent microscope photomicrographs showing the extent of DNA damage using comet assay in brain and liver tissues of the control group, the TMT group treated with 2.6 mg/kg TMT only once, the TMT-CSONEs group treated with 2.6 mg/kg TMT and treated with 100 mg/kg CSONEs one week before TMT and two weeks after TMT, TMT-Res group treated with 2.6 mg/kg TMT only once and treated with 5 mg/kg Res one week before TMT and two weeks after TMT. The TMT-Res-CSONEs group was treated with 2.6 mg/kg TMT only once and treated with 5 mg/kg Res-CSONEs one week before TMT and two weeks after TMT respectively at magnification (200x)

CSONEs groups, which reflects the positive effect of Res-CSONEs (Fig. 4 and 5).

In the liver tissue, most of the studied comet parameters were significantly (P<0.05) higher in the TMT group compared to all other groups. Moreover, the treatment with CSONEs and Res and Res-CSONEs significantly (P<0.05) protected the hepatic tissue against the hazardous effect of TMT, and Res-CSONEs possess the greatest advantage of all treated groups (Fig. 6).

Res-CSONEs reduced the expression of apoptotic and inflammatory genes

The mRNA expression levels of the apoptotic genes *Bax* and *Bcl2*, as well as the inflammatory gene *il-1β,* were assessed in the brains of all

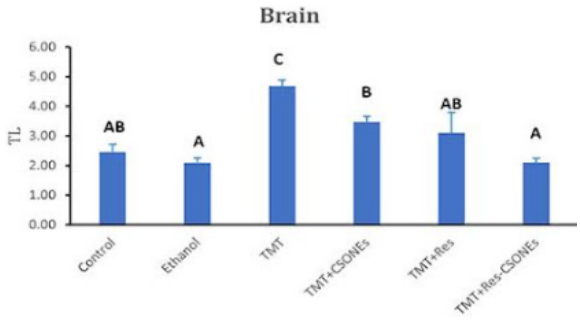

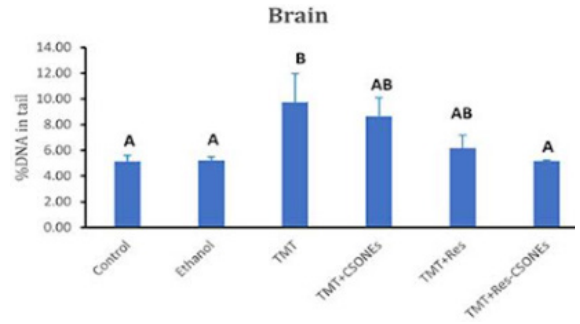

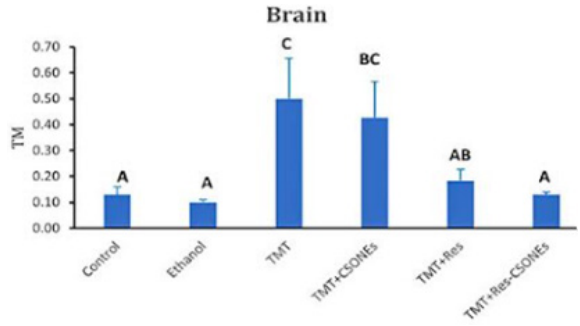

Fig. 5. The levels of tail length (TL), The percentage of DNA damage in the tail (%DNA), and the levels of the tail moment (TM) in the brain of the experimental groups. Data are displayed as mean ± standard error. Bars labeled with the same superscript letters are insignificantly (P>0.05) different, whereas those marked with different ones are significantly (P<0.05) different

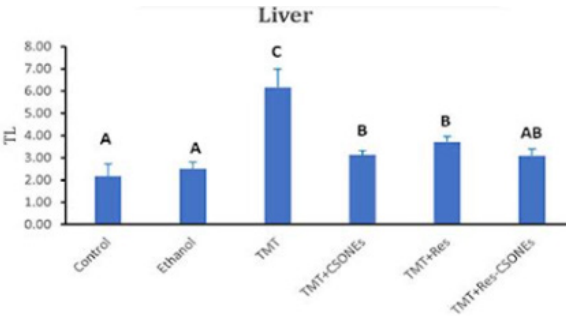

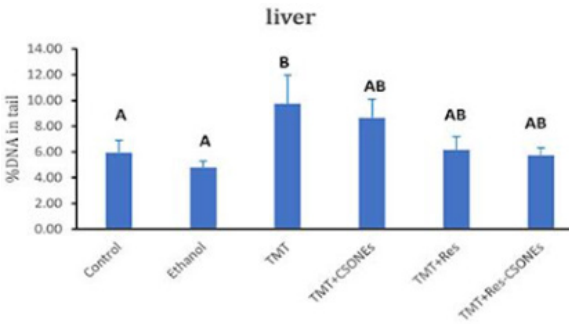

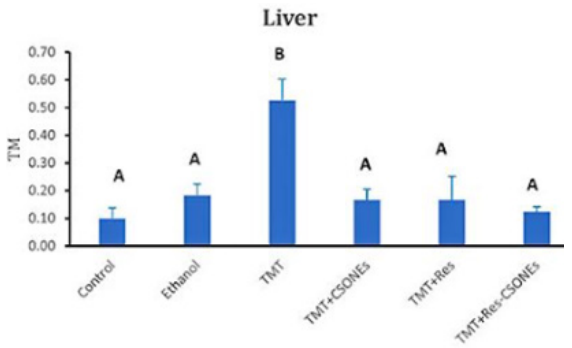

Fig. 6. The levels of tail length (TL), The percentage of DNA damage in the tail (%DNA), and the levels of the tail moment (TM) in the liver of all studied groups. Data are displayed as mean ± standard error. Bars labeled with the same superscript letters are insignificantly (P>0.05) different, whereas those marked with different ones are significantly (P<0.05) different

examined groups (Fig. 7). As compared to the control and ethanol groups, TMT treated group showed a significant decline (*P<0.05*) in the expression level of *Bcl2* associated with a significant (P<0.05) upregulation in the mRNA levels of *il-1β* and *Bax.* The mRNA levels of both *il-1β* and *Bax* of CSONEs, Res, and Res-CSONEs groups were significantly downregulated (P<0.05) compared to the TMT group. While the expression of the *Bcl2* gene was significantly upregulated in TMT+CSONEs, Res, and Res-CSONEs groups compared to the TMT group. Moreover, the expression of *Bcl2* was significantly different (*P<0.05*) in the Res-CSONEs group compared to the Res and CSONEs groups. However, there is an insignificant difference in the expression level of *Bax* in CSONEs, Res, and Res-CSONEs groups.

Res-CSONEs downregulated the expression of Tau protein

The expression level of Tau protein in the cortical and subiculum regions of the brain showed upregulation of Tau protein in the TMT-treated group compared to control and ethanol groups. In addition, there is a reduction in the expression level of Tau protein in CSONEs, Res,

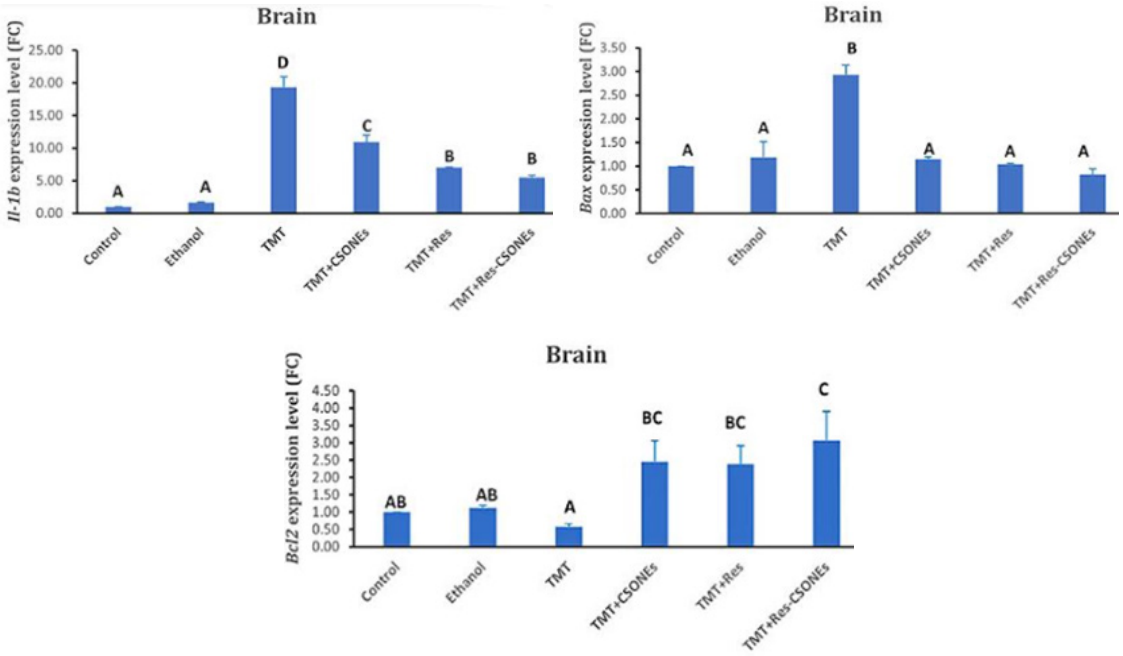

Fig. 7. Gene expression levels B-cell leukemia/lymphoma 2 (Bcl2), interleukin 1-beta (il-1β), and Bcl-2-associated X protein (Bax) in the brain of the experimental groups. Data are displayed as mean ± standard error. Bars labeled with the same superscript letters are insignificantly (P>0.05) different, whereas those marked with different ones are significantly (P<0.05) different

and Res-CSONEs compared to the TMT group. Moreover, the expression level of Tau protein was significantly reduced and eliminated in the subiculum region compared to the cortical region of the Res-CSONEs group Fig. 8.

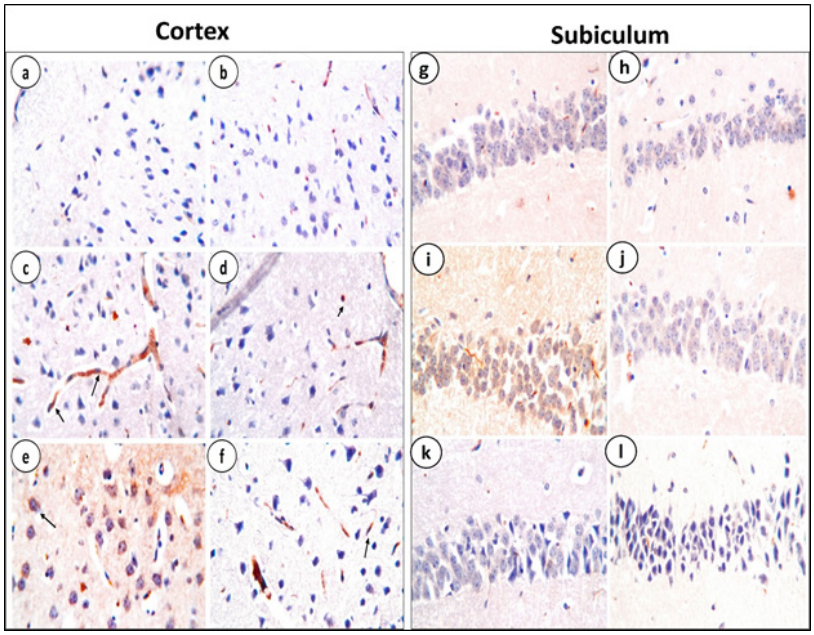

Fig. 8. Photomicrographs represent immunohistochemistry staining of Tau protein in cortex and subiculum regions. (a&g) the control group, (b&h) ethanol group. (c&i) The TMT group was treated with 2.6 mg/kg TMT only once. (d&j) the TMT-CSONEs group treated with 2.6 mg/kg TMT and treated with 100 mg/kg CSONEs one week before TMT and two weeks after TMT, (e&k) TMT-Res group treated with 2.6 mg/kg TMT only once and treated with 5 mg/kg Res one week before TMT and two weeks after TMT. (f&l) The TMT-Res-CSONEs group was treated with 2.6 mg/kg TMT only once and treated with 5 mg/kg Res-CSONEs one week before TMT and two weeks after TMT respectively at magnification (800x)

Res-CSONEs rehab histopathological alteration in brain

Microscopic examination of the cortical region of the brain showed no histopathological alteration and intact nuclear details and structures of the neurons in both normal control and treated ethanol groups (Fig. 9a-b) respectively, while TMT treated group showed degeneration in the neurons and some neurofibrillary tangles were seen (Fig. 9c). In addition, animals treated with TMT and CSONEs showed degeneration and pyknosis in some cortical neurons (Fig. 9d). The TMT-Res group showed degeneration in some neurons and some neurofibrillary tangles were seen (Fig. 9e). On the other hand, the animal group treated with TMT and Res-CSONEs showed degeneration in a few neurons and most neurons are intact (Fig. 9f).

Additionally, the histopathological examination of the subiculum region of the brain showed normal histological structure in the neurons in both normal control and treated ethanol groups (Fig. 10a-b) respectively, while TMT treated group showed degeneration in neurons and neurofibrillary tangles (Figu. 10c). Moreover, animals treated with TMT and CSONEs showed degeneration in a few neurons (Fig. 10d), in addition, the TMT-Res group showed degeneration in some neurons and few neurofibrillary tangles were seen (Fig. 10e).

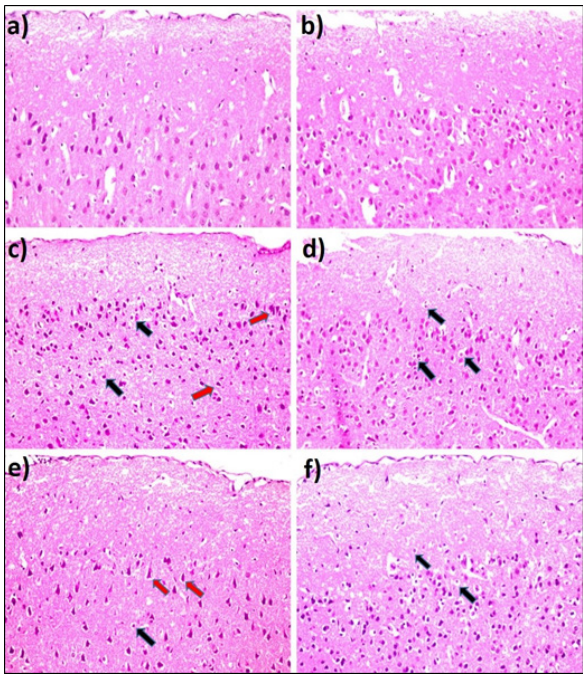

Fig. 9. Photomicrographs represent the brain cortex tissues of normal and treated groups of mice, (a) The normal control group showed no histopathological alteration and intact nuclear details in the neurons. (b) The treated group with 2% ethanol showed normal histological structure in the neurons. (c) The treated group with 2.6 mg/kg TMT only once showed nuclear pyknosis and degeneration in the neurons (black arrows) and some neurofibrillary tangles were detected (red arrows). (d) The treated group with 2.6 mg/kg TMT and treated with 100 mg/kg cumin seed oil nanoemulsion one week before TMT and two weeks after TMT showed some neurons had pyknosis and degeneration. (e) The treated group with 2.6 mg/kg TMT only once and treated with 5 mg/kg resveratrol one week before TMT and two weeks after TMT showed nuclear pyknosis and degeneration in some neurons (black arrows) and some neurofibrillary tangles were detected (red arrows). (f) The treated group with 2.6 mg/kg TMT only once and treated with 5 mg/kg resveratrol loaded cumin seed oil nanoemulsion one week before TMT and two weeks after TMT showed few neurons had nuclear pyknosis and degeneration (H & E X 400)

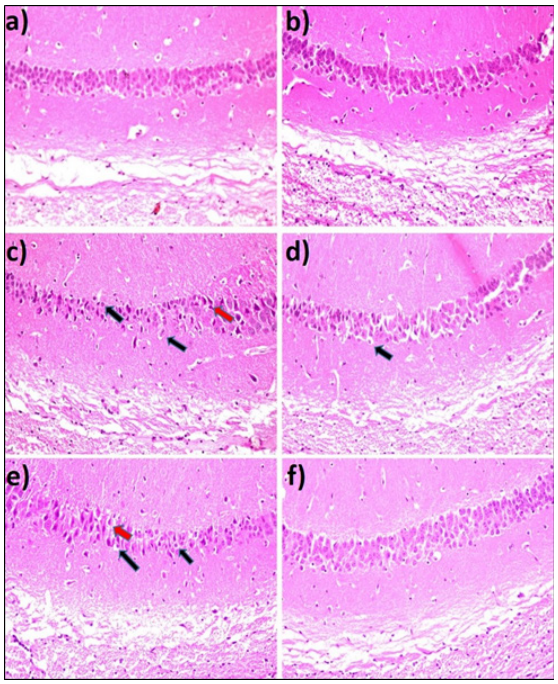

Fig. 10. Photomicrographs represent the brain subiculum tissues of normal and treated groups of mice, (a) The normal control group showed no histopathological alteration and intact nuclear details in the neurons. (b) The treated group with 2% ethanol showed normal histological structure in the neurons. (c) The treated group with 2.6 mg/kg TMT only once showed nuclear pyknosis and degeneration in some neurons (black arrows) and some neurofibrillary tangles were detected (red arrow). (d) The treated group with 2.6 mg/kg TMT and treated with 100 mg/kg cumin seed oil nanoemulsion one week before TMT and two weeks after TMT showed few neurons had pyknosis and degeneration. (e) The treated group with 2.6 mg/kg TMT only once and treated with 5 mg/kg resveratrol one week before TMT and two weeks after TMT showed nuclear pyknosis and degeneration in some neurons (black arrows) and few neurofibrillary tangles were detected (red arrows). (f) The treated group with 2.6 mg/kg TMT only once and treated with 5 mg/kg resveratrol-loaded cumin seed oil nanoemulsion one week before TMT and two weeks after TMT showed no histopathological alteration in the neurons (H & E X 400)

However, there is no histopathological alteration in the neurons in the animal group treated with TMT and Res-CSONEs (Fig. 10f).

Res-CSONEs ameliorate TMT effect in the liver

No histopathological alteration in liver tissues with the normal histological structure of the central vein and surrounding hepatocytes in the parenchyma in both normal control and ethanol-treated groups (Fig. 11a-b), respectively. In addition, TMT treated group showed dilatation of the portal vein and inflammatory cell infiltration surrounding the bile ducts in the portal area (Fig. 11c). Moreover, the animal group treated with TMT and CSONEs showed dilatation and hyperplasia in the bile ducts at the portal area (Figure 11d), while the animal group treated with TMT and Resveratrol showed few inflammatory cell infiltrations surrounding the bile duct in the portal area associated with dilatation in the portal vein (Fig. 11e). Finally, the animal group treated with TMT and Res-CSONEs showed hepatic parenchyma had degeneration in the hepatocytes and dilatation in the portal vein (Fig. 11f).

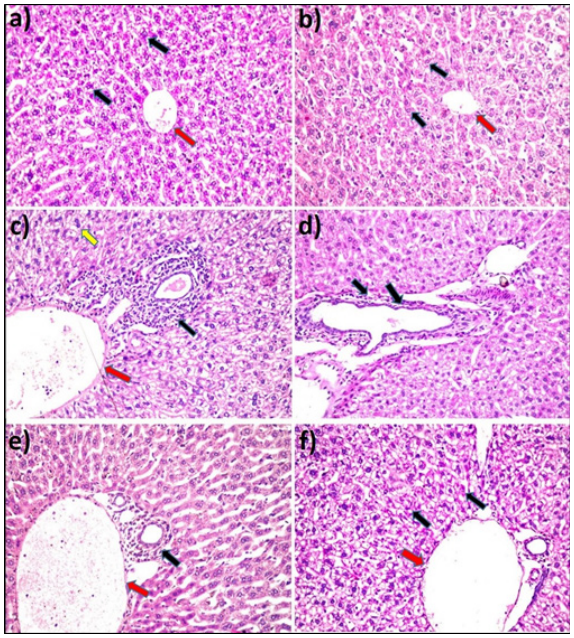

Figure 11. Photomicrographs represent the liver tissues of normal and treated groups of mice, (a) The normal control group showed the normal histological structure of the central vein (red arrows) and surrounding hepatocytes in the parenchyma (black arrows). (b) The treated group with 2% ethanol showed no histopathological alteration. (C) The treated group with 2.6 mg/kg TMT only once showed inflammatory cell infiltration surrounding the bile ducts at the portal area (black arrow) associated with dilatation of the portal vein (red arrow), degeneration in the hepatocytes in a diffuse manner and cells proliferation (yellow arrow). (D) The treated group with 2.6 mg/kg TMT and treated with 100 mg/kg cumin seed oil nanoemulsion one week before TMT and two weeks after TMT showed dilatation and hyperplasia in the bile ducts at the portal area. (E) The treated group with 2.6 mg/kg TMT only once and treated with 5 mg/kg resveratrol one week before TMT and two weeks after TMT showed few inflammatory cell infiltrations surrounding the bile duct in the portal area (black arrow) associated with dilatation in the portal vein (red arrow). (F) The treated group with 2.6 mg/kg TMT only once and treated with 5 mg/kg resveratrol-loaded cumin seed oil nanoemulsion one week before TMT and two weeks after TMT showed dilatation in the portal vein (red arrow) and hepatic parenchyma had degeneration in the hepatocytes (black arrow) (H & E X 400)

DISCUSSION

In the present study, we assessed the protective effect of resveratrol-loaded cumin seed oil nanoemulsions in mice with TMT-induced neurodegeneration. Res-CSONEs showed a more favorable neuroprotective effect on mice brain tissue than Res alone. Specifically, Res-CSONEs significantly decreased oxidative stress biomarkers and DNA damage parameters,Also it reduced the expression of *il-1β* and the apoptotic *Bax/Bcl2* ratio. Additionally, Res-CSONEs inhibited the aggregation of Tau protein in both the cortex and subiculum regions of the brain.

Several studies have shown the neuroprotective effects of Res due to its antioxidant and anti-inflammatory properties [44, 45]. However, Res has limitations due to its low bioavailability, poor water solubility, short half-life, and high photosensitivity [46]. To increase Res's solubility and bioavailability, we utilized CSONEs, which are known to enhance delivery to the brain due to their lipid nature. Additionally, the small size of this delivery system provides the added benefit of crossing the blood-brain barrier (BBB), ultimately improving the therapeutic effects of the drug [21].

Accordingly, small nanoemulsions were prepared from cumin seed oil by keeping the ratio of oil: Tween 80: water as 1: 2: 13, this ratio showed droplet size around 10 nm which was confirmed using TEM and DLS characterization techniques. While the size distribution of NEs was determined by dynamic light scattering (DLS) analysis exhibited a marginal increase in size compared to the corresponding dimensions observed in transmission electron microscopy (TEM) images. This divergence can be attributed to the distinct techniques used: DLS calculates the hydrodynamic diameter based on laser scattering

intensity, while TEM directly examines the sample using transmitted electron beams, offering an assessment of droplet size and shape [47]. Using small droplet size was important in our study as it enhances the penetration of the nanoemulsion through the BBB [48].

Moreover, in the current study, we selected a special essential oil to load Res, cumin seed oil extracted from the herbaceous plant Cuminum cyminum. Numerous studies illustrated its therapeutic effects such as hepatoprotective, neuroprotective, antioxidant, antistress, and anti-inflammatory properties [24-28]. Our study demonstrated that CSONEs have neuroprotective properties, as evidenced by their ability to reduce oxidative stress and DNA damage parameters, as well as to downregulate the expression of genes associated with apoptosis and inflammation, relative to the TMT groups. This is consistent with the previous studies illustrated the anti-inflammatory, and antioxidant effects of cumin seed oil [49-51].

The highly toxic substance Trimethyltin causes neurodegeneration by triggering oxidative stress, inflammation, and apoptosis [52]. Studies indicate that TMT raises ROS levels and hinders antioxidant enzymes, leading to oxidative damage in neurons [53]. Our data reported that TMT treatment increased the level of MDA, the end product of lipid peroxidation and decreased antioxidant enzymes GSH and SOD compared to the untreated group. On the other hand, Resveratrol acts as a free radical scavenger that removes ROS and reduces the level of MDA by inhibiting lipid peroxidation. Moreover, Resveratrol increases the activity of antioxidant enzymes [8]. Our data illustrated more advantages in the Res-CSONEs group than Res and CSONEs groups, which indicates the promising antioxidant effect of the Res-CSONEs drug formulation compared to Res alone.

TMT induces excessive free radical production, and ROS attacks DNA, resulting in the single or double-strand break, which leads to irreversible oxidative DNA damage [54-56]. Our data showed that TMT treatment increased all DNA damage parameters tail length (TL), % DNA, and tail moment (TM) in all examined tissues compared to the control group. On the other hand, Resveratrol can remove excess ROS and increase the activity of antioxidant enzymes, which inhibits oxidative DNA damage, reduces single and double-strand breakage of DNA, and promotes DNA repairing mechanisms [10]. Our findings are in acceptance with those of previous studies, which reported that Res, CSONEs, and Res-CSONEs treatment shows a significant decrease in all DNA damage parameters in all examined tissues compared to TMT treated group. The Res-CSONES group demonstrated a notable decrease in all DNA damage parameters in comparison to both the Res and CSONEs groups. The study confirms that loading Res on cumin seed oil provides synergistic benefits, resulting in enhanced biodistribution and improved crossing through the BBB for Res-CSONES. This is evidenced by the observed oxidative stress and DNA damage parameters.

Inflammation is a natural mechanism that helps the body defend against damage. Neuroinflammation is caused by the activation of astrocytes and microglia, as well as the release of inflammatory cytokines, which are related to neurodegenerative diseases [57]. TMT treatment induces neuroinflammation by activating microglia and astrocytes and releasing inflammatory cytokines such as *il-1β*, which affects neurons and leads to inflammatory injury and cell damage [58]. Our data showed a significant increase in the expression level of il-1β in all examined groups, especially in the TMT group compared to the untreated group. Resveratrol protects neurons against inflammatory injury and neuronal damage by reducing the production of pro-inflammatory cytokines like il-1β and inhibiting the activation of microglia, consistent with our findings [59].

As a result of increased ROS production, elevated MDA level, disruption of antioxidant enzymes, the incidence of DNA damage, and release of inflammatory cytokines because of TMT, all these events lead to neural injury and induction apoptosis. In our study, TMT increased the expression level of the pro-apoptotic gene Bax and decreased the expression of the anti-apoptotic gene Bcl2 and this agrees with the previous study of [60]. In contrast, Res can inhibit apoptosis by downregulating the pro-apoptotic gene Bax and upregulating the anti-apoptotic gene Bcl2 [61]. Our data is in line with previous findings, which showed Resveratrol treatment increases the expression level of anti-apoptotic gene Bcl2 and decreases the expression level of pro-apoptotic gene Bax resulting in inhibiting apoptosis and reducing neural damage. Moreover, both CSONES and Res-CSONEs showed a significant reduction in apoptotic genes due to a reduction in the Bax/Bcl2

ratio and therefore more protection of neuronal cells which indicates the advantages of new Res-CSONEs formulation.

Furthermore, the evaluation of tau protein in the brain (specifically the cortex and subiculum) using immunohistochemistry showed that the TMT-treated group had the highest accumulation of tau neurofibrillary tangles compared to the untreated group. This is consistent with previous studies that have indicated that TMT induces the phosphorylation of tau protein through the excessive production of ROS and increases the expression of inflammatory cytokines [62]. In contrast, Resveratrol has an anti-tauopathy effect, which reduces the aggregation and hyperphosphorylation of tau protein [63]. Our findings also agree with this, as we observed only a mild accumulation of tau neurofibrillary tangles in the Res, CSONEs, and Res-CSONEs groups.

ROS production causes oxidative stress, leading to damage to cell components and apoptosis associated with TMT neurotoxicity. TMT treatment results in nuclear pyknosis and degeneration of neurons, but Resveratrol, CSONEs, and Res-CSONEs decrease the number of degenerated neurons and improve neurological rehabilitation. Resveratrol restores damaged tissues by preventing apoptosis and necrosis, promoting neuron survival, and exhibiting antioxidant, anti-inflammatory, and antiapoptotic properties that were observed in the cortex and subiculum of the brain.

However, the histopathological examination revealed inflammatory cell infiltration and degeneration of hepatocytes in the liver, due to TMT treatment. Previous studies have reported that TMT toxicity causes oxidative stress, increases ROS and MDA production, DNA damage, inflammation, the release of inflammatory cytokines, upregulation of pro-apoptotic genes, and downregulation of anti-apoptotic genes leading to apoptosis and cell death [64, 65]. On the other hand, Res, CSONEs, and Res-CSONEs have hepatoprotective properties due to their antioxidant, anti-inflammatory, and anti-apoptotic effects [66]. The histopathological examination of liver tissue pretreated with Resveratrol showed improved tissue structure and a decrease in inflammatory cell infiltration.

CONCLUSION

Res-CSONEs have a better therapeutic impact than Res alone, which returns to the synergistic effect of both CSONEs and Res together. In addition, the Res-CSONEs lipid nature and small particle size were equal to 10 nm, which helped in the enhancement of Res-CSONEs biodistribution and crossing the blood-brain barrier. Res-CSONEs showed significant enhancement in neuronal cell homeostasis approved with a significant decrease in oxidative stress and DNA damage parameters, downregulation of inflammatory gene, and reduction in apoptotic *Bax/Bcl2* ratio that was accompanied by a reduction in Tau protein aggregation compared to Res alone. Moreover, the histopathological studies of both cortex and subiculum illustrated improved histological rehabilitation.

ACKNOWLEDGMENTS

The study experiments were conducted at the Genetics Laboratory, Department of Zoology at Cairo University, Giza, Egypt. Preparation of nanoemulsion and characterization was performed at Nanotechnology and Advanced Materials Central Lab, Agriculture Research Center, Egypt. The authors would like to thank Dr. Atef Ali for his assistance in performing the statistical analysis.

ETHICAL APPROVAL CONSENT TO PARTICIPATE

All experimental procedures were carried out following the national guidelines for the care and use of animals. The study was approved by the institutional animal care and use committee (IACUC) at faculty of science, Cairo University with approval number (CU/I/F/16/21).

CONSENT FOR PUBLICATION

None.

DATA AVAILABILITY

Raw data supporting the results reported in the manuscript are available from the authors.

FUNDING

None.

CONFLICTS OF INTEREST

The authors declare that they have no competing interests.

REFERENCES

1. International AsD. World Alzheimer Report 2021: Journey through the diagnosis of dementia. London Alzheimers Dis Int. 2021.

2. Organization WH. The top 10 causes of death. 9 December 2020. World Health Organization(20182020 https://www who int/news-room/fact-sheets/detail/the-top-10-causes of-death. 2021.

3. Dorsey E, Sherer T, Okun MS, Bloem BR. The emerging evidence of the Parkinson pandemic. J Parkinsons Dis. 2018;8(s1):S3-S8.
4. Yang W, Hamilton JL, Kopil C, Beck JC, Tanner CM, Albin RL, et al. Current and projected future economic burden of Parkinson's disease in the US. NPJ Parkinsons Dis. 2020;6(1):15.
5. Berman AY, Motechin RA, Wiesenfeld MY, Holz MK. The therapeutic potential of resveratrol: a review of clinical trials. NPJ Precis Oncol. 2017;1(1):35.
6. Rauf A, Imran M, Suleria HAR, Ahmad B, Peters DG, Mubarak MS. A comprehensive review of the health perspectives of resveratrol. Food Funct. 2017;8(12):4284-4305.
7. Rauf A, Imran M, Butt MS, Nadeem M, Peters DG, Mubarak MS. Resveratrol as an anti-cancer agent: A review. Crit Rev Food Sci Nutr. 2018;58(9):1428-1447.
8. Tellone E, Galtieri A, Russo A, Giardina B, Ficarra S. Resveratrol: a focus on several neurodegenerative diseases. Oxid Med Cell Longev. 2015;2015(1):392169.
9. Wang H, Jiang T, Li W, Gao N, Zhang T. Resveratrol attenuates oxidative damage through activating mitophagy in an in vitro model of Alzheimer's disease. Toxicol Lett. 2018;282:100-108.
10. Truong VL, Jun M, Jeong WS. Role of resveratrol in regulation of cellular defense systems against oxidative stress. Biofactors. 2018;44(1):36-49.
11. Wang Q, Liu Y, Zhou J. Neuroinflammation in Parkinson's disease and its potential as therapeutic target. Transl Neurodegener. 2015;4:1-9.
12. Francioso A, Mastromarino P, Masci A, d'Erme M, Mosca L. Chemistry, stability and bioavailability of resveratrol. Med Chem. 2014;10(3):237-245.
13. Wang S, Wang Z, Yang S, Yin T, Zhang Y, Qin Y, et al. Tissue distribution of trans-resveratrol and its metabolites after oral administration in human eyes. J Ophthalmol. 2017;2017(1):4052094.
14. Nirale P, Paul A, Yadav KS. Nanoemulsions for targeting the neurodegenerative diseases: Alzheimer's, Parkinson's and Prion's. Life Sci. 2020;245:117394.
15. Suyal J, Kumar B, Jakhmola V. Novel approach self-nanoemulsifying drug delivery system: a review. Advances in Pharmacology and Pharmacy. 2023;11(2):131-139.
16. Patel RP, Joshi JR. An overview on nanoemulsion: a novel approach. Int J Pharm Sci Res.2012;3(12):4640.
17. Sutradhar KB, Amin ML. Nanoemulsions: increasing possibilities in drug delivery. Eur J Nanomed. 2013;5(2):97 110.
18. Jaiswal M, Dudhe R, Sharma P. Nanoemulsion: an advanced mode of drug delivery system. 3 Biotech. 2015;5:123-127.
19. Patel D, Sawant KK. Self micro-emulsifying drug delivery system: formulation development and biopharmaceutical evaluation of lipophilic drugs. Curr Drug Deliv. 2009;6(4):419-424.
20. Singh Y, Meher JG, Raval K, Khan FA, Chaurasia M, Jain NK, et al. Nanoemulsion: Concepts, development and applications in drug delivery. J Control Release. 2017;252:28-49.
21. Locatelli FM, Kawano T, Iwata H, Aoyama B, Eguchi S, Nishigaki A, et al. Resveratrol-loaded nanoemulsion prevents cognitive decline after abdominal surgery in aged rats. J Pharmacol Sci. 2018;137(4):395-402.
22. Nirmala MJ, Durai L, Rao KA, Nagarajan R. Ultrasonic nanoemulsification of Cuminum cyminum essential oil and its applications in medicine. Int J Nanomedicine. 2020;795-807.
23. Fernandes SS, Egea MB, Salas-Mellado MdlM, Segura-Campos MR. Chia Oil and Mucilage Nanoemulsion: Potential Strategy to Protect a Functional Ingredient. Int J Mol Sci. 2023;24(8):7384.
24. Atli O, Can Karaca A, Ozcelik B. Encapsulation of Cumin (Cuminum cyminum L.) seed essential oil in the Chickpea Protein–Maltodextrin matrix. ACS Omega. 2023;8(4): 4156-4164.
25. Li R, Jiang ZT. Chemical composition of the essential oil of Cuminum cyminum L. from China. Flavour Fragr J. 2004;19(4):311-313.
26. Nostro A, Cellini L, Bartolomeo SD, Campli ED, Grande R, Cannatelli M, et al. Antibacterial effect of plant extracts against Helicobacter pylori. Phytother Res. 2005;19(3):198-202.
27. Gachkar L, Yadegari D, Rezaei MB, Taghizadeh M, Astaneh SA, Rasooli I. Chemical and biological characteristics of Cuminum cyminum and Rosmarinus officinalis essential oils. Food Chem. 2007;102(3):898-904.
28. Koppula S, Choi DK. Cuminum cyminum extract attenuates scopolamine-induced memory loss and stress-induced urinary biochemical changes in rats: a noninvasive biochemical approach. Pharm Biol. 2011;49(7):702-708.
29. Misiti F, Orsini F, Clementi ME, Lattanzi W, Giardina B, Michetti F. Mitochondrial oxygen consumption inhibition importance for TMT-dependent cell death in undifferentiated PC12 cells. Neurochem Int. 2008;52(6):1092-1099.
30. Geloso MC, Corvino V, Michetti F. Trimethyltin-induced hippocampal degeneration as a tool to investigate neurodegenerative processes. Neurochem Int. 2011;58(7):729-738.
31. Piacentini R, Gangitano C, Ceccariglia S, Fà AD, Azzena GB, Michetti F, et al. Dysregulation of intracellular calcium homeostasis is responsible for neuronal death in an experimental model of selective hippocampal degeneration induced by trimethyltin. J Neurochem. 2008;105(6):2109-2121.
32. Pompili E, Fabrizi C, Fumagalli L, Fornai F. Autophagy in trimethyltin-induced neurodegeneration. J Neural Transm. 2020;127:987-998.
33. Gong Q-H, Li F, Jin F, Shi J-S. Resveratrol attenuates neuroinflammation-mediated cognitive deficits in rats. J Health Sci. 2010;56(6):655-663.
34. Sheweita SA, El-Hosseiny LS, Nashashibi MA. Protective effects of essential oils as natural antioxidants against hepatotoxicity induced by cyclophosphamide in mice. PloS one. 2016;11(11):e0165667.
35. Frozza RL, Bernardi A, Paese K, Hoppe JB, Silva Td, Battastini AM, et al. Characterization of trans-resveratrol-loaded lipid-core nanocapsules and tissue distribution studies in rats. J Biomed Nanotechnol. 2010;6(6):694-703.
36. Sönmez Ü, Sönmez A, Erbil G, Tekmen I, Baykara B. Neuroprotective effects of resveratrol against traumatic brain injury in immature rats. Neurosci Lett. 2007;420(2):133-137.
37. Ohkawa H, Ohishi N, Yagi K. Assay for lipid peroxides in animal tissues by thiobarbituric acid reaction. Anal Biochem. 1979;95(2):351-358.
38. Beutler E, Duron O, Kelly BM. Improved method for the determination of blood glutathione. J Lab Clin Med. 1963;61:882-888.
39. Nishikimi M, Rao NA, Yagi K. The occurrence of superoxide anion in the reaction of reduced phenazine methosulfate and molecular oxygen. Biochem Biophys Res Commun. 1972;46(2):849-854.
40. Tice RR, Agurell E, Anderson D, Burlinson B, Hartmann A, Kobayashi H, et al. Single cell gel/comet assay: guidelines for *in vitro* and *in vivo* genetic toxicology testing. Environ Mol Mutagen. 2000;35(3):206-221.
41. Nandhakumar S, Parasuraman S, Shanmugam M, Rao KR, Chand P, Bhat BV. Evaluation of DNA damage using single-cell gel electrophoresis (Comet Assay). J Pharmacol Pharmacother. 2011;2(2):107.

42. Gad HA, Mansour M, Abbas H, Malatani RT, Khattab MA, Elmowafy E. "Plurol will not miss the boat": A new manifesto of galantamine conveyance. J Drug Deliv Sci Technol. 2022;74:103516.
43. Bancroft JD, Layton C, Suvarna SK. Bancroft's theory and practice of histological techniques: Churchill Livingstone Elsevier. 2013.
44. Rocha-González HI, Ambriz-Tututi M, Granados-Soto V. Resveratrol: a natural compound with pharmacological potential in neurodegenerative diseases. CNS Neurosci Ther. 2008;14(3):234-247.
45. Andrade S, Ramalho MJ, Pereira MdC, Loureiro JA. Resveratrol brain delivery for neurological disorders prevention and treatment. Front pharmacol. 2018;9:1261.
46. Amri A, Chaumeil J, Sfar S, Charrueau C. Administration of resveratrol: what formulation solutions to bioavailability limitations? J Control Release. 2012;158(2):182-193.
47. ElZorkany HE, El-Shorbagy HM, Farroh KY, Youssef T, Sabet S, Salaheldin TA. Monitoring the cellular uptake of silica-coated CdSe/ZnS quantum dots by time lapse confocal laser scanning microscopy. J Appl Pharm Sci. 2018;8(3):001-008.
48. Rehman S, Md S, Baboota S, Ali J. Analyzing nanotheraputics-based approaches for the management of psychotic disorders. J Pharmacol Sci. 2019;108(12):3757-3768.
49.Wei J, Zhang X, Bi Y, Miao R, Zhang Z, Su H. Anti-inflammatory effects of cumin essential oil by blocking JNK, ERK, and NF-κB signaling pathways in LPS-stimulated RAW 264.7 cells. Evid Based Complement Alternat Med. 2015;2015(1):474509.
50. Platel K, Srinivasan K. Influence of dietary spices and their active principles on pancreatic digestive enzymes in albino rats. Food/Nahrung. 2000;44(1):42-46.
51. Topal U, Sasaki M, Goto M, Otles S. Chemical compositions and antioxidant properties of essential oils from nine species of Turkish plants obtained by supercritical carbon dioxide extraction and steam distillation. Int J Food Sci Nutr. 2008;59(7-8):619-634.
52. Ghofrani S, Joghataei M-T, Afshin-Majd S, Baluchnejadmojarad T, Roghani M. Crocin, a bioactive constituent of Crocus sativus, alleviates trimethyltin-induced cognitive deficits through down-regulation of hippocampal apoptosis and oxidative stress. J basic clin pathophysiol.2022;10(1):38-44.
53. Shin E-J, Suh S, Lim Y, Jhoo W-K, Hjelle O, Ottersen O,et al. Ascorbate attenuates trimethyltin-induced oxidative burden and neuronal degeneration in the rat hippocampus by maintaining glutathione homeostasis. Neuroscience. 2005;133(3):715-727.
54. Wang X, Cai J, Zhang J, Wang C, Yu A, Chen Y, et al. Acute trimethyltin exposure induces oxidative stress response and neuronal apoptosis in Sebastiscus marmoratus. Aquat Toxicol. 2008;90(1):58-64.
55. Farghaly AA, Abo-Zeid MA. Protective effect of vitamin C on trimethyltin induced DNA damage using comet assay and chromosomal aberrations. Cytologia. 2010;75(3):229-236.
56. Kang D-H. Oxidative stress, DNA damage, and breast cancer. AACN Adv Crit Care. 2002;13(4):540-549.
57. Liu W, Tang Y, Feng J. Cross talk between activation of microglia and astrocytes in pathological conditions in the central nervous system. Life Sci. 2011;89(5-6):141-146.
58. Gunasekar PG, Mickova V, Kotyzova D, Li L, Borowitz JL, Eybl V, et al. Role of astrocytes in trimethyltin neurotoxicity. J Biochem Mol Toxicol. 2001;15(5):256-262.
59. Meng T, Xiao D, Muhammed A, Deng J, Chen L, He J. Anti-inflammatory action and mechanisms of resveratrol. Molecules. 2021;26(1):229.
60. Jeong E-S, Bajgai J, You I-S, Rahman M, Fadriquela A, Sharma S, et al. Therapeutic effects of hydrogen gas inhalation on trimethyltin-induced neurotoxicity and cognitive impairment in the C57BL/6 mice model. Int J Mol Sci. 2021;22(24):13313.
61. Hou Y, Wang K, Wan W, Cheng Y, Pu X, Ye X. Resveratrol provides neuroprotection by regulating the JAK2/STAT3/PI3K/AKT/mTOR pathway after stroke in rats. Genes Dis. 2018;5(3):245-255.
62. Park SB, Kang JY, Kim JM, Park SK, Park SH, Kang JE, et al. Aruncus dioicus var. kamtschaticus extract suppresses mitochondrial apoptosis induced-neurodegeneration in trimethyltin-injected ICR mice. J Food Biochem. 2018;42(6):e12667.
63. Pasinetti GM, Wang J, Ho L, Zhao W, Dubner L. Roles of resveratrol and other grape-derived polyphenols in Alzheimer's disease prevention and treatment. Biochim Biophys Acta Mol Basis Dis. 2015;1852(6):1202-1208.
64. Liu X-J, Wang Y-Q, Shang S-Q, Xu S, Guo M. TMT induces apoptosis and necroptosis in mouse kidneys through oxidative stress-induced activation of the NLRP3 inflammasome. Ecotoxicol Environ Saf. 2022;230:113167.
65. Wang Y, Liu X, Jing H, Ren H, Xu S, Guo M. Trimethyltin induces apoptosis and necroptosis of mouse liver by oxidative stress through YAP phosphorylation. Ecotoxicol Environ Saf. 2022;248:114327.
66. Chupradit S, Bokov D, Zamanian MY, Heidari M, Hakimizadeh E. Hepatoprotective and therapeutic effects of resveratrol: A focus on anti-inflammatory and antioxidative activities. Fundam Clin Pharmacol. 2022;36(3):468-485.